ENVIRONMENTAL RESEARCH
LETTERS

LETTER • OPEN ACCESS

# Distinct roles of land cover in regulating spatial variabilities of temperature responses to radiative effects of aerosols and clouds

To cite this article: Linyi Wei *et al* 2021 *Environ. Res. Lett.* **16** 124070

ENVIRONMENTAL RESEARCH
LETTERS

OPEN ACCESS

RECEIVED
29 March 2021

REVISED
11 November 2021

ACCEPTED FOR PUBLICATION
1 December 2021

PUBLISHED
16 December 2021



LETTER

# Distinct roles of land cover in regulating spatial variabilities of temperature responses to radiative effects of aerosols and clouds

**Linyi Wei[1], Yong Wang[1,*], Shu Liu[1], Guang J Zhang[2] and Bin Wang[1,3,4]**

[1] Department of Earth System Science, Ministry of Education Key Laboratory for Earth System Modeling, Institute for Global Change Studies, Tsinghua University, Beijing 100084, People's Republic of China
[2] Scripps Institution of Oceanography, La Jolla, CA, United States of America
[3] State Key Laboratory of Numerical Modelling for Atmospheric Sciences and Geophysical Fluid Dynamics, Institute of Atmospheric Physics, Chinese Academy of Sciences, Beijing, People's Republic of China
[4] College of Earth and Planetary Sciences, University of Chinese Academy of Sciences, Beijing, People's Republic of China
[*] Author to whom any correspondence should be addressed.

**E-mail:** yongw@mail.tsinghua.edu.cn

**Keywords:** land cover, aerosol radiative effects, cloud radiative effects, temperature response

Supplementary material for this article is available online

## Abstract

Surface temperature responses to radiative perturbations due to aerosols and clouds are complicated by the land surface properties. To disentangle these complexities, this study, from a terrestrial surface energy budget perspective, isolates the underlying biophysical processes from the instantaneous radiative effects of aerosols and clouds on surface temperature using the National Center for Atmospheric Research Community Earth System Model version 1.2.1. It is found that in comparison with the global heterogeneous distributions of instantaneous radiative perturbations at the surface induced by aerosols and clouds, the spatial variations of the corresponding surface temperature responses to aerosol direct radiative effects (DRE) during the daytime and cloud radiative effects (CRE) during the nighttime are amplified. It is because of the consistent global distribution of the local surface climate sensitivity (a function of land cover properties such as surface roughness and Bowen ratio) with those of daytime DRE and nighttime CRE. By applying identical anthropogenic aerosol and precursor emissions over eight major past, present and projected future anthropogenic aerosol emitting regions (i.e. Brazil, China, East Africa, India, Indonesia, South Africa, United States and Western Europe), surface temperature responses to aerosol radiative cooling in the daytime and cloud radiative warming in the nighttime over these regions positively regulated by local surface climate sensitivities are prominent.

## 1. Introduction

Atmospheric aerosols and clouds have substantial impacts on climate (Coakley *et al* 1983, Arking 1991, Charlson *et al* 1992, Tiedtke 1993, Garrett and Zhao 2006, Zhao and Garrett 2015, Li *et al* 2019, Zhao *et al* 2020a). They can affect the radiation budget at the surface by absorbing and scattering solar radiation (Bohren and Huffman 1983, Arking 1991, Hartmann 1993, Forster *et al* 2007). Due to the short lifetime of aerosols in the atmosphere, the spatial heterogeneous distribution of aerosol emissions largely determine the spatial distributions of atmospheric aerosol loading and thus aerosol direct radiative effects (DRE) (Taylor and Penner 1994, Shindell 2014, Yang *et al* 2016, Persad and Caldeira 2018). Similar to aerosols, heterogeneous spatial distributions also exist in cloud fraction and cloud hydrometeors which are modulated by atmospheric states and underlying surface heat fluxes (Chen *et al* 2019, Grabowski and Prein 2019, Zhao *et al* 2019, Yang *et al* 2020, Sun *et al* 2021). These spatial distributions control the spatial distribution of cloud radiative effects (CRE). Meanwhile, aerosols and clouds can influence each other: aerosols can act as cloud condensation nuclei and ice nuclei to alter cloud albedo and lifetime (Albrecht 1989, Twomey 1977, 1991, Ramanathan 2001, Wang *et al* 2014) while clouds affect the aerosol concentrations

in the atmosphere via many routes such as hygroscopic growth (Sun *et al* 2019, Zhao *et al* 2020b) and wet scavenging (Loosmore and Cederwall 2004, Wang *et al* 2021). Therefore, their interactions further complicate the spatial variability of the surface radiation perturbations and associated surface temperature responses.

Land cover has large spatial variations as well (Chiang *et al* 2018) with diverse natural and anthropogenic land types (e.g. bareland, forest and cropland). With surface properties such as surface albedo, surface roughness, Bowen ratio (sensible heat flux divided by latent heat flux) (Li *et al* 2019), the underlying surface dynamics and thermodynamics exchange energy, momentum, and substance with the atmosphere to influence the global and regional climate (Sellers *et al* 1997, Shepherd 2006, Lee *et al* 2011, Sterling *et al* 2013, Zhao *et al* 2014, Findell *et al* 2017, Shen and Zhao 2020, Shen *et al* 2021). As a result, surface temperature responds to land surface energy dissipation (Juang *et al* 2007, Luyessart *et al* 2014, Li *et al* 2019). For instance, tropical forests and urban areas compared to other land surfaces can efficaciously redistribute the energy due to the rough surface and intense turbulence resulting in weak temperature changes (Chakraborty and Lee 2019, Chakraborty *et al* 2021b). With historical land use and land cover change (LULCC), the contributions of changes in different land cover types to local temperature responses via non-radiative processes are quantified (Bright *et al* 2017). Nonetheless, even for a given land surface type (e.g. forest and urban area), the local temperature response to its change still can vary in different regions due to different local background climates (Lee *et al* 2011, Zhao *et al* 2014).

As the surface temperature is influenced by both instantaneous aerosol DRE and CRE, and the underlying biophysical processes, there are few studies disentangling these complexities. Most previous studies regarding the impacts of aerosol DRE and CRE on surface temperature in different regions neglected the essential role of the spatial heterogeneity of land cover types (e.g. Persad and Caldeira 2018). This will screen some valuable guidelines for policy making and climate projections in terms of a combination of anthropogenic aerosol emission control and LULCC in the future. Chakraborty and Lee (2019) isolated the direct surface longwave and shortwave radiative effects of aerosols from the Modern-Era Retrospective Analysis for Research and Applications, Version 2 (MERRA-2) reanalysis data and calculated the related spatial surface temperature sensitivities. They found higher surface temperature sensitivity for the longwave component which is driven by a combination of the spatial variabilities of aerosols and biophysical control of the underlying surface. The reduced global mean diurnal temperature range (DTR) due to the contrasting longwave and shortwave effects of aerosols is largely contributed by anthropogenic aerosols.

As the magnitude of CRE is much larger than that of aerosol DRE (Boucher *et al* 2013), it is important to elucidate the spatial variability of the surface temperature response to instantaneous CRE combined with the underlying biophysical processes, and explore how it is different from the land cover regulations to the aerosol DRE-induced temperature response. Moreover, since the anthropogenic aerosol origin compared with the natural counterpart plays a more vital role in diurnal temperature variation (Chakraborty and Lee 2019), how the surface temperature response differs over major past, present and projected future anthropogenic aerosol emission regions with divergent land cover and different background climate. To explore these, this study isolates the role of land cover from individual surface temperature changes directly caused by instantaneous aerosol and cloud radiative perturbations at the surface over the globe using the theory of the intrinsic biophysical mechanism (IBPM; Lee *et al* 2011) with a global climate model.

## 2. Methods

### 2.1. Climate model

The global climate model used in this study is the National Center for Atmospheric Research (NCAR) Community Earth System Model version 1.2.1 (CESM1.2.1) whose atmospheric model, the Community Atmosphere Model version 5.3 (CAM5.3), and land model, the Community Land Model version 4 (CLM4), are relevant for the study. In CAM5.3, a finite volume dynamical core is used. As for physical processes, deep convection, shallow convection, stratiform cloud microphysics, boundary layer moist turbulence and radiative transfer are parameterized by Zhang and McFarlane (1995), Park and Bretherton (2009), Morrison and Gettelman (2008), Bretherton and Park (2009), and Iacono *et al* (2008), respectively. The properties and processes of major aerosol species (mineral dust, sulfate, sea salt, black carbon, primary organic matter and secondary organic aerosol) are treated in the Modal Aerosol Module (MAM) (Liu *et al* 2012). The aerosol size distribution is represented by three lognormal modes (MAM3): Aitken, accumulation and coarse modes. The associated mass mixing ratios of different aerosol components and the number concentration in each mode are predicted. Spatial land surface heterogeneity is represented by CLM4. For each land grid, the land surface consists of multiple land units (i.e. wetland, glacier, lake, vegetated, and urban), snow/soil columns, and up to 16 possible plant functional types (Oleson and Bonan 2000, Bonan *et al* 2002). Surface energy and water balance variables in the non-urban and urban land units are parameterized by a standard natural land

surface model and an urban surface model, respectively.

### 2.2. Experiments

Differing in anthropogenic aerosol emissions only, ten Atmospheric Model Intercomparison Project type simulations at a horizontal resolution of 1.9° × 2.5° and 30 vertical levels are performed using prescribed, seasonally varying present-day (PD) (climatologically averaged from 1981 to 2001) sea surface temperatures and sea ice concentrations (Hurrell *et al* 2008). Other forcings such as solar radiation, greenhouse gas concentration and land cover are all fixed at PD climatological conditions. All simulations are run for six years and the last five years are used for analysis. Among the ten simulations (table S1 (available online at stacks.iop.org/ERL/16/124070/mmedia)), there are two experiments under pre-industrial (PI) and PD climatological aerosol and aerosol-precursor emissions, respectively. The other eight simulations are conducted using the PI climatological emissions with the exceptions over the following regions respectively: Brazil, China, East Africa, India, Indonesia, South Africa, United States and Western Europe. In these regions, the same PD climatological aerosol and aerosol-precursor emissions as those over China are used (Persad and Caldeira 2018). These eight key geopolitical regions have distinct climate regimes (Kottek *et al* 2006) (figure S1) and land cover (figure S2). Western Europe and the United States as major anthropogenic aerosol emitting areas in the past historical period are under mid-latitude temperate and snow climate zones. Western Europe is mainly covered by forests and croplands followed by grasslands, while the United States mainly features grasslands, shrublands, forests and barelands. India and China, current major emitting regions, are under temperate and partly arid climate zones dominantly covered by multiple land cover types (e.g. croplands, forests, barelands and grasslands). Indonesia, Brazil, East Africa, and South Africa are grouped into the future potential major emitting regions. Their main land cover types and climate regimes differ. Indonesia and Brazil both are rich in forests and are of the equatorial climate with vigorous convection and much precipitation while East Africa and South Africa are in the arid climate zone where vegetation-scarce grasslands and baerlands exist abundantly.

### 2.3. IBPM theory

The IBPM theory proposed by Lee *et al* (2011) solves for surface temperature responses to surface radiative forcing via isolating atmospheric feedbacks ($\Delta T_{s,\mathrm{rad}}$) (see supplementary text S1 for details):

$$\Delta T_{s,\mathrm{rad}} = \lambda^* (\Delta S + \Delta L_{\downarrow}) \tag{1}$$

where $\Delta$ indicates the perturbation signal due to aerosols or clouds, $S$ is the instantaneous surface net shortwave flux, $L_{\downarrow}$ is the instantaneous surface incoming longwave flux. Following Ghan (2013) and Ghan *et al* (2012), $\Delta S$ and $\Delta L_{\downarrow}$ due to aerosols and clouds are estimated as $S(L_{\downarrow}) - S(L_{\downarrow})_{\mathrm{clean}}$ and $S(L_{\downarrow})_{\mathrm{clean}} - S(L_{\downarrow})_{\mathrm{clean,\,clear}}$ respectively. Here $S(L_{\downarrow})_{\mathrm{clean}}$ are diagnostic surface radiative fluxes but neglecting absorption and scattering of radiation by atmospheric aerosols, while $S(L_{\downarrow})_{\mathrm{clean,\,clear}}$ are additional diagnostic surface radiative fluxes with absorption and scattering of radiation by both atmospheric aerosols and clouds (including aerosol indirect effects) neglected.

The effective local climate sensitivity $\lambda^*$, which is linked with the surface radiation budget and the atmospheric feedback, is the modification of the intrinsic climate sensitivity $\lambda_0$ in equation (3) given by differentiating the Stefan-Boltzmann equation (Council 2003, Bright *et al* 2017):

$$\lambda^* = \frac{\lambda_0}{1+f} \tag{2}$$

$$\lambda_0 = \frac{1}{4\sigma T_s^3} \tag{3}$$

where $\sigma$ is the Stefan-Boltzmann constant, $T_s$ is surface temperature, $f$, a dimensionless energy redistribution factor, is a measure of the efficiency of energy dissipation between the surface and the lower atmosphere having the form:

$$\begin{aligned} f &= \frac{\lambda_0}{T_s - T_a}(H + \mathrm{LE}) = \rho C_p \frac{1+\frac{1}{\beta}}{r_a 4\sigma T_s^3} \\ &\approx \frac{\lambda_0}{T_s - T_a}\left(S + L_{\downarrow} - \sigma T_s^4\right) \\ &\approx \frac{\lambda_0}{T_s - T_a}\left(S + L_{\downarrow} - \sigma T_a^4\right) - 1 \end{aligned} \tag{4}$$

where $T_a$ is the air temperature at the reference height, $r_a$ is surface roughness, $H$ is sensible heat flux and LE is latent heat flux and $\beta$ is the Bowen ratio.

To quantify the temperature responses by instantaneous aerosol DRE and CRE, the IBPM mechanism introduces the local climate sensitivity ($\lambda^*$) on behalf of the energy redistribution efficacy based on the underlying land surface. There are several assumptions and approximations, including the blackbody hypothesis of the Earth, the zero approximation of small values, the omitted climate sensitivity over the ocean and Antarctic surfaces, and the single radiative model of ground surface balance with the lower atmosphere.

As seen in equation (1), the surface temperature responses to instantaneous surface radiation perturbations due to aerosols and clouds ($\Delta T_{s,\mathrm{rad}}$) can be isolated from the total surface temperature changes ($\Delta T_s$) which consists of $\Delta T_a$, $\Delta T_{s,\mathrm{rad}}$ and $\Delta T_{s,f}$. $\Delta T_a$ is the change of background air temperature caused by atmospheric processes. $\Delta T_{s,f}$ is the temperature change due to LULCC and other factors, which alter surface roughness, sensible and latent heat

fluxes (Lee *et al* 2011, Zhao *et al* 2014, Bright *et al* 2017). Unless otherwise stated, the surface temperature change/response throughout the text is $\Delta T_{s,\,rad}$ rather than the total surface temperature change ($\Delta T_s$). Aerosols and clouds also have impacts on temperature responses by perturbing $f$ ($\Delta T_{s,\,f}$) via a non-radiative pathway (see supplementary text S1) (Chakraborty *et al* 2021a, 2021b). With the fixed effective local climate sensitivity $\lambda^*$ from the PD simulation (see supplementary text S1), these impacts have been eliminated.

## 3. Results

### 3.1. Model evaluation

Since the effective local climate sensitivity $\lambda^*$, and the perturbations of net shortwave radiation and incoming longwave radiation at the surface due to aerosols and clouds are used to calculate $\Delta T_{s,\,rad}$, the realism of them in the PD simulation is evaluated first. Statistical metrics such as the coefficient of determination ($R^2$), the root mean square error (RMSE) and the mean bias error (MBE) are used. As shown in table S2, the simulated net shortwave radiation and incoming longwave radiation at global land surfaces in all- and clear-sky conditions (used for deriving CRE) agree well with MERRA-2 reanalysis, showing $R^2$ values between 0.8 and 0.9. When comparing with the Clouds and the Earth's Radiant Energy System observations, the values of $R^2$ further climb beyond 0.95. For surface net shortwave radiation and incoming longwave radiation in clean- and clear-sky conditions used for deriving aerosol DRE, the values of $R^2$ are 0.85 and 0.93, respectively. For the global mean, the modeled values for these variables all fall in the uncertain ranges of the observations and reanalysis, showing MBE values are much smaller than the observational uncertainties. Compared with the global means in observations/reanalysis, the RMSE values of the modeled variables are striking as well. As for the simulated $\lambda^*$ tightly linked with land cover types, the global distributions in the daytime and nighttime (see figure 1 below) resemble those in MERRA-2 although the magnitudes are smaller (Chakraborty and Lee 2019). Furthermore, other terms in the surface energy budget such as sensible and latent heat fluxes with CLM have been shown to agree well with observations (Chakraborty *et al* 2021b). Note that even if using a different surface attribution method (two-resistance mechanism including both the aerodynamic and surface resistance, TRM) (Li *et al* 2019), its local climate sensitivity and temperature responses due to aerosol DRE and CRE resemble those calculated by IBPM (figure S3).

### 3.2. Spatial variability of temperature response in the PD simulation

The surface climate sensitivity can be regarded as an indicator of land cover type because it describes the energy redistribution process between the surface and the lower troposphere by turbulence which is largely dependent on the surface roughness and Bowen ratio. As shown in figures 1(a) and (b), the surface climate sensitivity $\lambda^*$ for both daytime and nighttime is lower over areas with high surface roughness and low Bowen ratio (e.g. forests) than over areas with low surface roughness and high Bowen ratio (e.g. arid and polar regions). It implies that the lower sensitivity of surface temperature to surface radiative perturbations results from stronger turbulent mixing transporting more energy to the lower troposphere. As turbulence in the planetary boundary layer weakens at night, the nighttime $\lambda^*$ becomes ~twice larger than that in the daytime.

Following equation (1), local surface temperature responses ($\Delta T_{s,\,rad}$) to instantaneous aerosol DRE are modulated by the local surface climate sensitivity. As for instantaneous aerosol DRE in the PD simulation, over the arid zone such as the Sahara Desert, Arabian Peninsula and northwestern China with heavy dust loading, strong aerosol DRE along with high local surface climate sensitivities lead to the largest surface temperature changes all over the world by up to −1 K for daytime and 0.3 K for nighttime (figures 1(c)–(f)). In contrast, small temperature responses are found over regions with abundant forests such as Amazon and Congo where aerosol DRE levels are even comparable with those in high air polluted areas (e.g. South Asia), suggesting an increasingly important role of the underlying biophysical processes as the local surface climate sensitivity decreases (figures 1(c)–(f) and S4). Overall, since the maxima of aerosol DRE are over arid and semi-arid regions (e.g. Sahara) where the maxima of the local climate sensitivity also exist, land cover, to some degree, enhances the spatial variation (measured by $\left(\frac{\sigma}{\mu}\right)^2$ where $\mu$ is the global mean and $\sigma$ is the standard deviation) of the temperate response to aerosol DRE compared to the spatial variation of aerosol DRE itself especially during the day (1.89 in the temperature response versus 1.15 in aerosol DRE) (figures 1(c) and (e)).

As for CRE, it is climatologically several times larger than aerosol DRE in magnitude especially over the regions with both aerosols and clouds in abundance, so the CRE-induced surface temperature changes ($\Delta T_{s,\,rad}$) are more pronounced than those by aerosol DRE (figures 1(g)–(j)). For instance, the largest CRE (in magnitude) emerges over tropical rainforests with abundant aerosols from wildfire and volatile organic compounds, and vigorous convection. Nonetheless, as these regions are linked with the lowest $\lambda^*$, the temperature responses to CRE there are mediated mostly by more than −2.0 and up to 1.0 K for daytime and nighttime, respectively. In comparison, the polar regions of the Northern Hemisphere and the Tibetan Plateau have the largest temperature

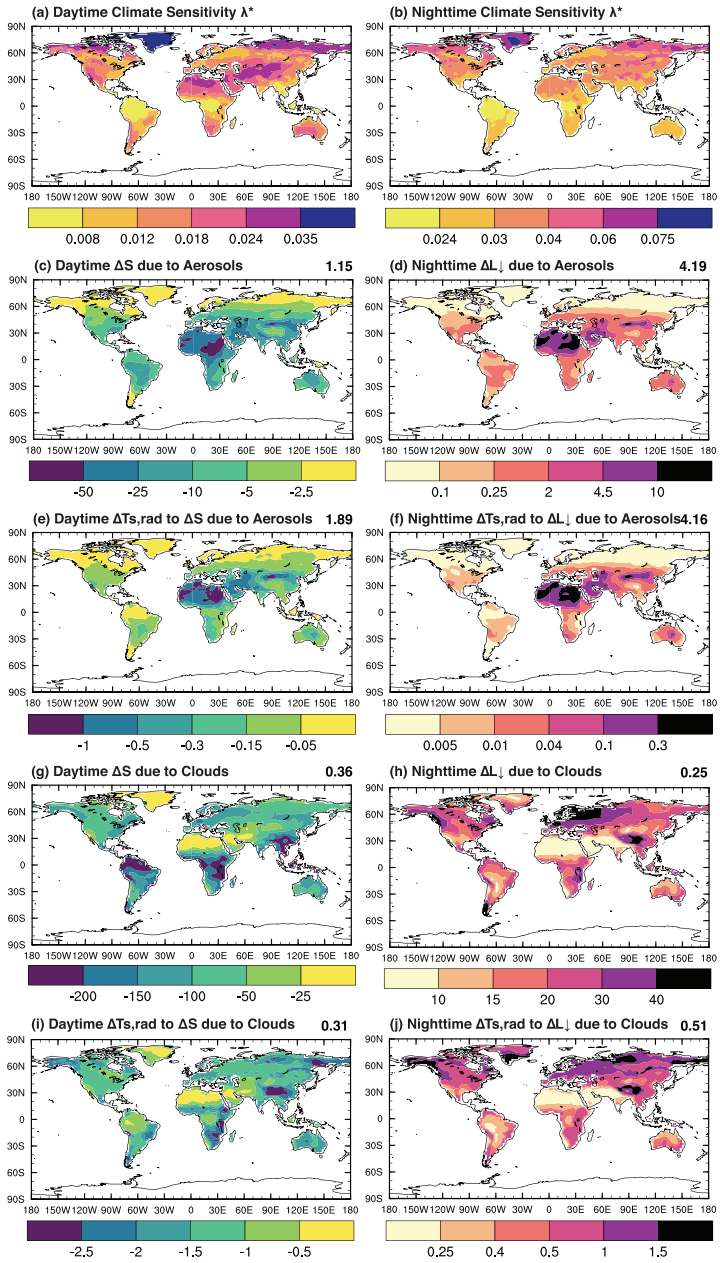


**Figure 1.** Global distributions of (a) daytime and (b) nighttime surface climate sensitivity (K W $m^{-2}$), (c) daytime shortwave radiative effect (RE) due to aerosols (W $m^{-2}$), (d) nighttime longwave RE due to aerosols (W $m^{-2}$), (e) daytime temperature perturbation due to aerosol shortwave RE (K), (f) nighttime temperature perturbation due to aerosol longwave RE (K), (g) daytime shortwave RE due to clouds (W $m^{-2}$), (h) nighttime longwave RE due to clouds (W $m^{-2}$), (i) daytime temperature perturbation due to cloud shortwave RE (K), and (j) nighttime temperature perturbation due to cloud longwave RE (K) in the PD simulation. Numbers on the upper right corner in (c)–(j) are the values of $\left(\frac{\sigma}{\mu}\right)^2$ measuring the magnitude of the spatial variation.

responses while the values of CRE there are moderate. Over arid regions such as Sahara, high surface climate sensitivities amplify the weak CRE effects on the temperature responses. In this regard, different from aerosol DRE where land cover enlarges the spatial variation of the temperate response, land cover plays an opposite role in CRE during the day (0.31 in CRE smaller than 0.36 in the corresponding temperature response, figures 1(g) and (i)). However, for nighttime, the consistent relationships between the surface climate sensitivity and the radiative forcing in the middle and high latitudes conversely increase the spatial discrepancy of the temperature response (0.51 in the temperature response larger than 0.25 in CRE, figures 1(h) and (j).

For aerosol DRE and CRE, both have the contrasting effects of shortwave and longwave radiation on surface temperature. As cooling by the shortwave radiation effect overwhelms warming by the longwave radiation effect (figure 1), the daily averaged temperatures to aerosol DRE and CRE have decreased accordingly (figure S5). The change of the

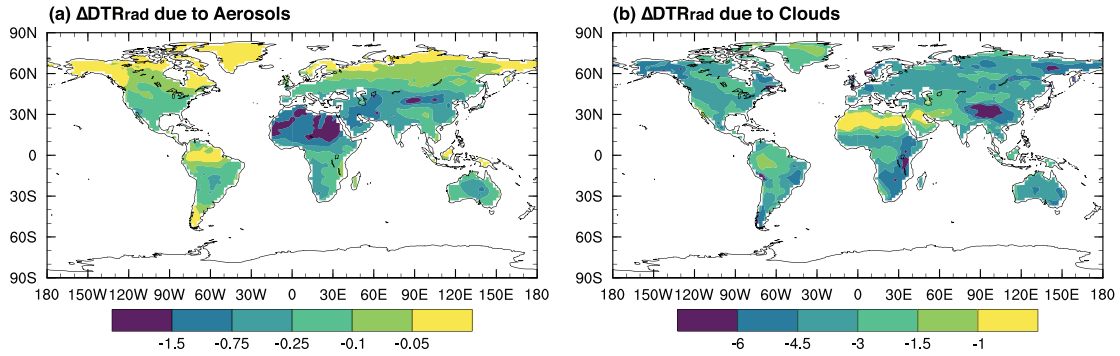


**Figure 2.** Global distributions of diurnal temperature range changes ($\Delta DTR_{rad}$; in K) due to (a) aerosol DRE and (b) CRE in the PD simulation.

local diurnal temperature range (DTR, defined as the temperature difference between the daily maximum and minimum temperatures) due to aerosol DRE and CRE ($DTR_{rad}$) is reduced accordingly due to the cooling during the day and the warming during the night for both aerosol DRE and CRE (figure 2). One exception is that over the high-latitudes when solar radiation is weak, the net effect of CRE during the daytime is warming having ~4.38 W $m^{-2}$ in the simulations, which is consistent with Garrett and Zhao (2006), Zhao and Garrett (2015).

### 3.3. Local temperature response in the identical aerosol emission simulations

Local temperature changes ($\Delta T_{s,rad}$) over major anthropogenic aerosol emission regions in the past, present and future projections (i.e. Brazil, China, East Africa, India, Indonesia, South Africa, United States and Western Europe) to the identical anthropogenic aerosol emissions but individually with distinct natural aerosols in the background are explored. Diverse land cover-associated local climate sensitivities have been shown over the eight regions (e.g. high vegetation canopies with low climate sensitivities over Brazil and Indonesia) (figure 3). As mentioned above, arid regions such as East Africa due to the small aerosol wet removal rate and the large local dust emissions have large local aerosol burdens and associated aerosol DRE (figures 3(a) and (b)). Coupling with the large surface climate sensitivity there, East Africa experiences larger temperature changes to aerosol DRE than other regions for both daytime and nighttime. However, humid regions such as Brazil and Indonesia due to frequent aerosol wet scavenging by light rain from vigorous convection (Wang *et al* 2021) have small aerosol burdens and associated aerosol DRE even with the same anthropogenic aerosol emissions as in China. With their low surface climate sensitivities, the corresponding temperature responses to aerosol DRE are still as low as those in the PD simulation. Also because of low surface climate sensitivities, despite frequent convection over Indonesia and Brazil (Tan *et al* 2015), CRE-induced temperature responses there are smaller than or comparable with those of arid regions where clouds are scarce (figures 3(c) and (d)).

More essential regulations of diverse land surfaces represented by different surface climate sensitivities on surface temperature responses are found in aerosol DRE during daytime and CRE at night (figure 3). Specifically, with local daytime aerosol DRE from −22.0 to −7.3 W $m^{-2}$, higher surface climate sensitivity generally corresponds to larger surface temperature response showing $R^2 = 0.53$ in linear regression (figure 3(a)). Similarly, for CRE during the nighttime, the temperature response is tightly controlled by land cover with $R^2 = 0.53$ in linear regression (figure 3(d)). Both of them pass the significance test with a 95% confidence level. In contrast, during the day for aerosol DRE and the night for CRE, the regulation role of land cover weakens showing $R^2 = 0.05$ and $R^2 = 0.11$ in linear regression, respectively (figures 3(c) and (d)). Similar results can be obtained by performing the analysis at all grids over eight regions (figure S6).

With anthropogenic aerosol burdens (represented by the differences between the eight sensitivity simulations and the PI simulation) (figures S7–S9) from the identical anthropogenic aerosol emissions, the regional temperature responses to anthropogenic aerosol DRE and CRE are investigated as well. A stronger dependence of daytime temperature responses on land cover is found to anthropogenic aerosol DRE than to anthropogenic aerosol CRE (figure S10).

The local DTR changes due to aerosol DRE and CRE in eight regions vary with the temperature responses during the day and the night. DTR changes to aerosol DRE (from −0.73 to −0.06 K) (figure 4(a)) are much smaller than those to CRE (−4.0 ~ −2.0 K) (figure 4(b)). As for local daily temperature changes (figure S11), the values due to CRE are about twofold—fivefold larger than those due to aerosol DRE. For instance, the largest decrease due to clouds can be as much as −0.8 K (emerge over Indonesia) while that due to aerosols is just around −0.2 K (emerge over South Africa). The land cover

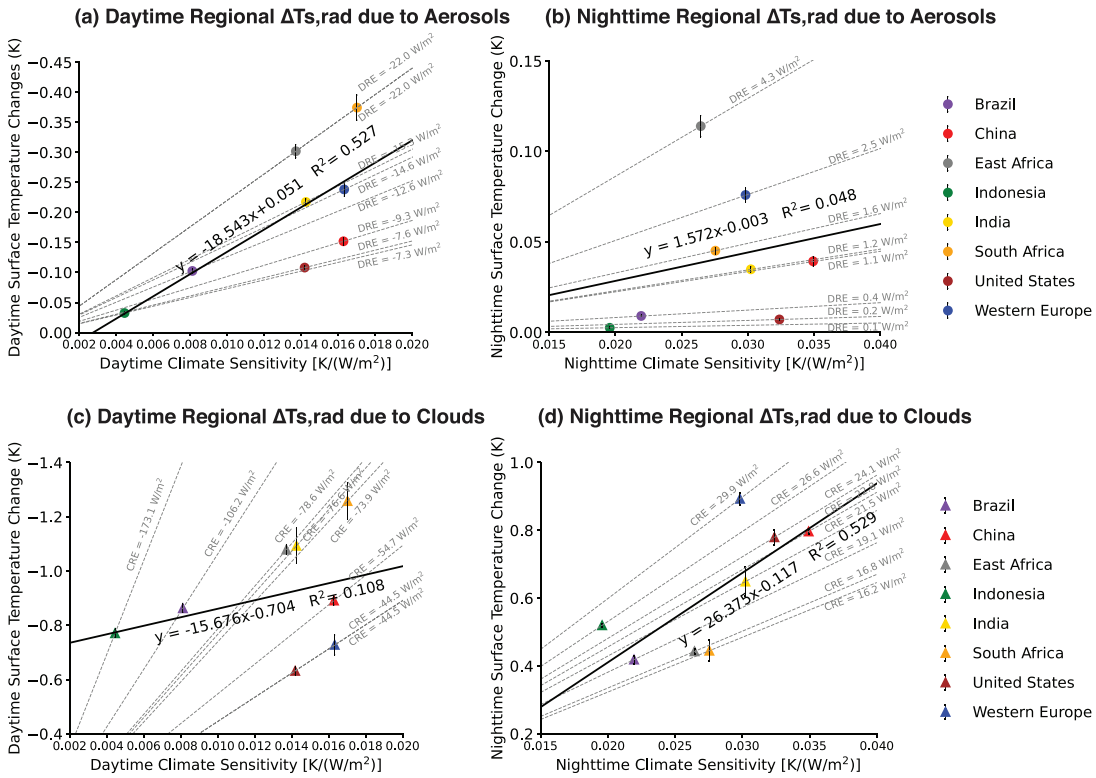


**Figure 3.** Regional surface temperature responses $\Delta T_{s,\,rad}$ due to (a) and (b) aerosol DRE and (c) and (d) CRE (a) and (c) during daytime and (b) and (d) nighttime in the eight sensitivity simulations. The error bar is the annual standard deviation, the grey dashed line represents the regional radiative forcing, and the black solid line indicates the linear regression for the eight regions. The linear relationships in (a), (c) and (d) are significant at a 95% confidence level.

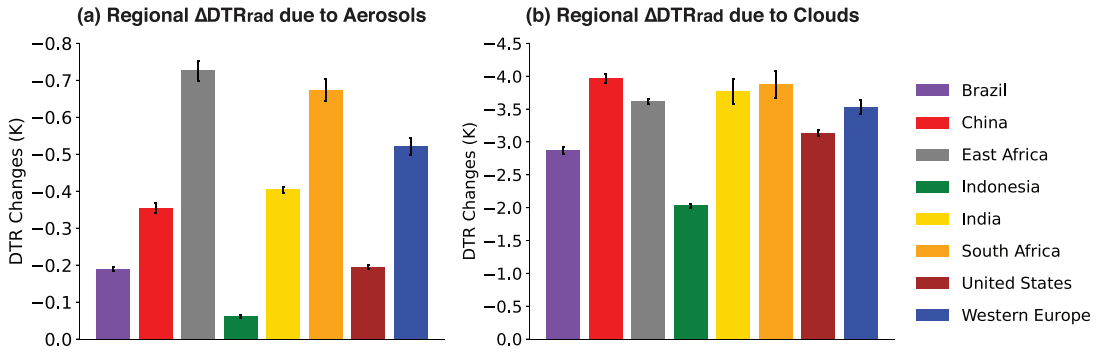


**Figure 4.** Changes in regional diurnal temperature ranges $\Delta DTR_{rad}$ due to (a) aerosol DRE and (b) CRE in the eight sensitivity simulations. The error bar represents the annual standard deviation.

type associated surface climate sensitivity modulates the DTR change more systematically to aerosol DRE than to CRE. In arid regions such as East Africa and South Africa, the largest aerosol DRE along with the highest climate sensitivity decrease the DTR there substantially, while in Brazil and Indonesia, the lower climate sensitivity counteracts the impact of aerosol DRE on the DTR changes. However, the DTR changes to CRE are relatively more identical to the identical anthropogenic aerosol emissions. Thus, as a response to the identical anthropogenic aerosol emissions, the DTR changes to aerosol DRE over the eight regions differmore than those to CRE.

## 4. Discussion and conclusions

Previous studies on the impact of aerosol-cloud-climate interactions on surface temperature ($\Delta T_s$) (Ackerman *et al* 2000, Ramanathan 2001, Lelieveld *et al* 2002, Sun and Zhao 2020, Deng *et al* 2021) overlook the role of land surface types in different background climates (e.g. Persad and Caldeira 2018). This study focuses on how land cover regulates instantaneous aerosol DRE and CRE related changes in surface temperature ($\Delta T_{s,\,rad}$) over the global land surfaces and isolates the role of land cover from these complicated processes using the NCAR CESM1.2.1 through

the lens of surface energy balance. Some original findings below are obtained.

Compared to the spatial variabilities of aerosol DRE and CRE land cover enlarges the spatial variation of the associated temperature responses to aerosol DRE during the daytime and CRE during the nighttime respectively while it narrows down that of the temperature response to CRE during the daytime. The opposite effects of land cover on the surface temperature responses to aerosol DRE and CRE during the daytime can be largely attributed to the contrasting collocations of local surface climate sensitivity and aerosol DRE and CRE. i.e. the arid regions with large aerosol DRE and large surface climate sensitivity versus the humid regions with large CRE and small surface climate sensitivity.

With identical anthropogenic aerosol emissions over Brazil, China, East Africa, India, Indonesia, South Africa, United States and Western Europe which represent major past, present and projected future emitting regions, local temperature responses to aerosol DRE (CRE) are strongly regulated by land cover in the daytime (nighttime). For temperature responses to anthropogenic aerosols, a stronger dependence of daytime temperature responses on land cover is found to anthropogenic aerosol DRE than to anthropogenic aerosol CRE. It suggests that the spatial variation of the impact of anthropogenic aerosols on surface temperature is mainly through anthropogenic aerosol DRE rather than anthropogenic aerosol CRE.

The findings in this study have important implications for a combination of future LULCC and anthropogenic aerosol emission changes. For example, future emission centers such as Brazil and Indonesia will feature the greater potential for surface temperature responses because they are also the centers of urban expansion and deforestation (due to increasing local climate sensitivity). As mentioned in the methods, besides the radiative pathway, aerosols and clouds can impact local surface temperature via the non-radiative pathway. In Chakraborty *et al* (2021b), aerosols can induce strong local cooling by enhancing surface evapotranspiration. Therefore, it is worthy of quantification of the individual non-radiative contributions of clouds and aerosols to local surface temperature changes in the future.

## Data availability statement

The data that support the findings of this study are openly available. And the CAM5 datasets for all plots are provided in an open repository Zenodo (https://doi.org/10.5281/zenodo.5229277).

## Acknowledgments

YW is supported by the National Natural Science Foundation of China Grant 41975126 and the National Key Research and Development Program of China Grant 2017YFA0604000. GJZ is supported by the Department of Energy, Office of Science, Biological and Environmental Research Program (BER), under Award Number DE-SC0019373. We thank the five reviewers for the comments which significantly improve the quality of the paper.

## References

Ackerman A S, Toon O B, Stevens D E, Heymsfield A J, Ramanathan V and Welton E J 2000 Reduction of tropical cloudiness by soot *Science* **288** 1042

Albrecht B A 1989 Aerosols, cloud microphysics, and fractional cloudiness *Science* **245** 1227

Arking A 1991 The radiative effects of clouds and their impact on climate *Bull. Am. Meteorol. Soc.* **72** 795–814

Bohren C F and Huffman D R 1983 Absorption and Scattering by an Arbitrary Particle. *Absorption and Scattering of Light by Small Particles* (Chichester: Wiley Science Paperback Series) 57–81

Bonan G B, Levis S, Kergoat L and Oleson K W 2002 Landscapes as patches of plant functional types: an integrating concept for climate and ecosystem models *Glob. Biogeochem. Cycles* **16** 5-1-5-23

Boucher O *et al* 2013 Clouds and aerosols *Climate Change 2013: The Physical Science Basis. Contribution of Working Group I to the Fifth Assessment Report of the Intergovernmental Panel on Climate Change* ed S Solomon *et al* (Cambridge: Cambridge University Press) 571–632

Bretherton C S and Park S 2009 A new moist turbulence parameterization in the community atmosphere model *J. Clim.* **22** 3422–48

Bright R M, Davin E, O'Halloran T, Pongratz J, Zhao K and Cescatti A 2017 Local temperature response to land cover and management change driven by non-radiative processes *Nat. Clim. Change* **7** 296–302

Chakraborty T C and Lee X 2019 Land cover regulates the spatial variability of temperature response to the direct radiative effect of aerosols *Geophys. Res. Lett.* **46** 8995–9003

Chakraborty T C, Lee X and Lawrence D M 2021b Strong local evaporative cooling over land due to atmospheric aerosols *J. Adv. Model. Earth Syst.* **13** e2021MS002491

Chakraborty T C, Sarangi C and Lee X 2021a Reduction in human activity can enhance the urban heat island: insights from the COVID-19 lockdown *Environ. Res. Lett.* **16** 054060

Charlson R J, Schwartz S E, Hales J M, Cess R D, Coakley J A, Hansen J E and Hofmann D J 1992 Climate forcing by anthropogenic aerosols *Science* **255** 423–30

Chen J, Wu X, Yin Y, Lu C, Xiao H, Huang Q and Deng L 2019 Thermal effects of the surface heat flux on cloud systems over the Tibetan Plateau in boreal summer *J. Clim.* **32** 4699–714

Chiang W S, Georgi D, Yildirim T, Chen J H and Liu Y 2018 A non-invasive method to directly quantify surface heterogeneity of porous materials *Nat. Commun.* **9** 784

Coakley J A, Cess R D and Yurevich F B 1983 The effect of tropospheric aerosols on the earth's radiation budget: a parameterization for climate models *J. Atmos. Sci.* **40** 116–38

Council N R 2003 *Understanding Climate Change Feedbacks* (Washington, DC: *The National Academies* ) pp 166

Deng W, Cohen J, Wang S and Lin C 2021 Improving the understanding between climate variability and observed extremes of global $NO_2$ over the past 15 years *Environ. Res. Lett.* **16** 054020

Findell K L, Berg A, Gentine P, Krasting J P, Lintner B R, Malyshev S, Santanello J A and Shevliakova E 2017 The

impact of anthropogenic land use and land cover change on regional climate extremes *Nat. Commun.* **8** 989
Forster P *et al* 2007 Changes in atmospheric constituents and in radiative forcing *Climate Change 2007: The Physical Science Basis. Contribution of Working Group I to the 4th Assessment Report of the Intergovernmental Panel on Climate Change* ed S Solomon *et al* (Cambridge: Cambridge University Press) 131–217
Garrett T J and Zhao C 2006 Increased Arctic cloud longwave emissivity associated with pollution from mid-latitudes *Nature* **440** 787–9
Ghan S J 2013 Technical Note: estimating aerosol effects on cloud radiative forcing *Atmos. Chem. Phys.* **13** 9971–4
Ghan S J, Liu X, Easter R C, Zaveri R, Rasch P J, Yoon J H and Eaton B 2012 Toward a minimal representation of aerosols in climate models: comparative decomposition of aerosol direct, semidirect, and indirect radiative forcing *J. Clim.* **25** 6461–76
Grabowski W W and Prein A F 2019 Separating dynamic and thermodynamic impacts of climate change on daytime convective development over land *J. Clim.* **32** 5213–34
Hartmann D L 1993 Chapter 6 radiative effects of clouds on earth's climate *International Geophysics* ed P V Hobbs (New York: Academic) pp 151–73
Hurrell J W, Hack J J, Shea D, Caron J M and Rosinski J 2008 A new sea surface temperature and sea ice boundary dataset for the community atmosphere model *J. Clim.* **21** 5145–53
Iacono M J, Delamere J S, Mlawer E J, Shephard M W, Clough S A and Collins W D 2008 Radiative forcing by long-lived greenhouse gases: calculations with the AER radiative transfer models *J. Geophys. Res. Atmos.* **113** D13
Juang J-Y, Katul G, Siqueira M, Stoy P and Novick K 2007 Separating the effects of albedo from eco-physiological changes on surface temperature along a successional chronosequence in the southeastern United States *Geophys. Res. Lett.* **34** L21408
Kottek M, Grieser J, Beck C, Rudolf B and Rubel F 2006 World map of the Köppen-Geiger climate classification updated *Meteorol. Z.* **15** 259–63
Lee X *et al* 2011 Observed increase in local cooling effect of deforestation at higher latitudes *Nature* **479** 384–7
Lelieveld J *et al* 2002 Global air pollution crossroads over the mediterranean *Science* **298** 794
Li D, Liao W, Rigden A J, Liu X, Wang D, Malyshev S and Shevliakova E 2019 Urban heat island: aerodynamics or imperviousness *Sci. Adv.* **5** eaau4299
Li Z *et al* 2019 East Asian Study of Tropospheric Aerosols and their Impact on Regional Clouds, Precipitation, and Climate (EAST-AIR$_{CPC}$) *J. Geophys. Res. Atmos.* **124** 13026–54
Liu X *et al* 2012 Toward a minimal representation of aerosols in climate models: description and evaluation in the community atmosphere model CAM5 *Geosci. Model Dev.* **5** 709–39
Loosmore G A and Cederwall R T 2004 Precipitation scavenging of atmospheric aerosols for emergency response applications: testing an updated model with new real-time data *Atmos. Environ.* **38** 993–1003
Luyssaert S *et al* 2014 Land management and land-cover change have impacts of similar magnitude on surface temperature *Nat. Clim. Change* **4** 389–93
Morrison H and Gettelman A 2008 A new two-moment bulk stratiform cloud microphysics scheme in the community atmosphere model, version 3 (CAM3). Part I: description and numerical tests *J. Clim.* **21** 3642–59
Oleson K W and Bonan G B 2000 The effects of remotely sensed plant functional type and leaf area index on simulations of boreal forest surface fluxes by the ncar land surface model *J. Hydrometeorol.* **1** 431–46
Park S and Bretherton C S 2009 The University of Washington shallow convection and moist turbulence schemes and their impact on climate simulations with the community atmosphere model *J. Clim.* **22** 3449–69
Persad G G and Caldeira K 2018 Divergent global-scale temperature effects from identical aerosols emitted in different regions *Nat. Commun.* **9** 3289
Ramanathan V 2001 Aerosols, climate, and the hydrological cycle *Science* **294** 2119–24
Sellers P J *et al* 1997 Modeling the exchanges of energy, water, and carbon between continents and the atmosphere *Science* **275** 502–9
Shen L and Zhao C 2020 Dominance of Shortwave Radiative Heating in the Sea-Land Breeze Amplitude and its Impacts on Atmospheric Visibility in Tokyo, Japan *J. Geophys. Res. Atmos.* **125** e2019JD031541
Shen L, Zhao C and Yang X 2021 Climate-driven characteristics of sea-land breezes over the globe *Geophys. Res. Lett.* **48** e2020GL092308
Shepherd J M 2006 Evidence of urban-induced precipitation variability in arid climate regimes *J. Arid Environ.* **67** 607–28
Shindell D T 2014 Inhomogeneous forcing and transient climate sensitivity *Nat. Clim. Change* **4** 274–7
Sterling S M, Ducharne A and Polcher J 2013 The impact of global land-cover change on the terrestrial water cycle *Nat. Clim. Change* **3** 385–90
Sun W, Wang B, Wang Y, Zhang G J, Han Y, Wang X and Yang M 2021 Parameterizing subgrid variations of land surface heat fluxes to the atmosphere improves boreal summer land precipitation simulation with the NCAR CESM1.2 *Geophys. Res. Lett.* **48** e2020GL090715
Sun Y and Zhao C 2020 Influence of Saharan Dust on the Large-Scale Meteorological Environment for Development of Tropical Cyclone Over North Atlantic Ocean Basin *J. Geophys. Res. Atmos.* **125** e2020JD033454
Sun Y, Zhao C, Su Y, Ma Z, Li J, Letu H, Yang Y and Fan H 2019 Distinct impacts of light and heavy precipitation on PM2.5 mass concentration in Beijing *Earth Space Sci.* **6** 1915–25
Tan J, Jakob C, Rossow W B and Tselioudis G 2015 Increases in tropical rainfall driven by changes in frequency of organized deep convection *Nature* **519** 451–4
Taylor K E and Penner J E 1994 Response of the climate system to atmospheric aerosols and greenhouse gases *Nature* **369** 734–7
Tiedtke M 1993 Representation of clouds in large-scale models *Mon. Weather Rev.* **121** 3040–61
Twomey S A 1991 Aerosols, clouds and radiation *Atmos. Environ. A* **25** 2435–42
Twomey S 1977 The influence of pollution on the shortwave albedo of clouds *J. Atmos. Sci.* **34** 1149
Wang Y, Liu X, Hoose C and Wang B 2014 Different contact angle distributions for heterogeneous ice nucleation in the community atmospheric model version 5 *Atmos. Chem. Phys.* **14** 10411–30
Wang Y, Xia W, Liu X, Xie S, Lin W, Tang Q, Ma H, Jiang Y, Wang B and Zhang G J 2021 Disproportionate control on aerosol burden by light rain *Nat. Geosci.* **14** 72–76
Yang X, Zhao C, Zhou L, Wang Y and Liu X 2016 Distinct impact of different types of aerosols on surface solar radiation in China *J. Geophys. Res. Atmos.* **121** 6459–71
Yang Y, Zhao C and Fan H 2020 Spatiotemporal distributions of cloud properties over China based on Himawari-8 advanced Himawari imager data *Atmos. Res.* **240** 104927
Zhang G J and McFarlane N A 1995 Sensitivity of climate simulations to the parameterization of cumulus convection in the Canadian climate centre general circulation model *Atmos. Ocean* **33** 407–46
Zhao C, Chen Y, Li J, Letu H, Su Y, Chen T and Wu X 2019 Fifteen-year statistical analysis of cloud characteristics over China using Terra and Aqua moderate resolution imaging spectroradiometer observations *Int. J. Climatol.* **39** 2612–29

Zhao C and Garrett T J 2015 Effects of Arctic haze on surface cloud radiative forcing *Geophys. Res. Lett.* **42** 557–64
Zhao C, Yang Y, Fan H, Huang J, Fu Y, Zhang X, Kang S, Cong Z, Letu H and Menenti M 2020a Aerosol characteristics and impacts on weather and climate over the Tibetan Plateau *Natl Sci. Rev.* **7** 492–5
Zhao L, Lee X, Smith R B and Oleson K 2014 Strong contributions of local background climate to urban heat islands *Nature* **511** 216–9
Zhao X, Sun Y, Zhao C and Jiang H 2020b Impact of precipitation with different intensity on $PM_{2.5}$ over typical regions of China *Atmosphere* **11** 906